

## STRAIN LOCALISATION IN THERMOELECTRIC COMPONENTS BY LASER PROBE SHEAROGRAPHY

S. Jorez, S. Dilhaire, L. Patino Lopez, S. Grauby, W. Claeys.

CPMOH – Université de Bordeaux 1351 Cours de la Libération 33405 Talence Cedex – France  
K-I. Uemura

ITTJ – 10-35, Mihanayama, Tsuzuki-ku, Yokohama-shi 224-0066 – Japan  
J.G. Stockholm

MARVEL THERMOELECTRICS – 11, rue Joachim du Bellay, F-78540 Vernouillet – France

### Abstract

We have developed an original optical set-up and method for the measurement of strain in electronic components. We have applied it for the study of thermoelectric devices. The method is based on speckle interferometry [1-2] imaging called shearography [3-5]. Two images of a same object lighted by coherent laser light are recorded upon a CCD camera through an appropriate optical system. The two images are slightly shifted one with respect to the other. This allows determining the gradient of normal surface displacement in the direction of the shift. Information taken in this manner in several directions allows to derive a map of a parameter related to the surface displacement gradients that we call "fragility factor".

### 1. Introduction

The determination of thermomechanical stress induced in thermoelectric coolers is a crucial issue for their reliability. Powerful simulation tools exist and are often based upon finite element computer work; they allow a good description of the thermomechanical effects induced in electronic devices. The validity of such a simulation work has to be experimentally proven as it depends on the physical effects taken into account and upon the thermal and mechanical constants used. Measurements upon real devices can therefore not be passed round.

The purpose of the present work is to propose an optical contactless measuring technique of the thermomechanical strain in thermoelectric coolers. The method, called shearography [3-4], is based on speckle interferometry, it allows measuring the strain induced in running devices and localizing the regions of maximum energy deformation [5-6] approximated by what we call the fragility factor.

### 2 Shearography

#### 2.1 Principle of the method.

Shearing interferometry is based on a special imaging of a device illuminated by coherent light. Two images of the same sample, slightly shifted one with respect to the other, are recorded upon a CCD camera. Each pixel intensity results from interferences between lights coming from two shifted points of the device. Due to the running or to the mechanical stress, the surface of the device moves inducing changes upon the images recorded by the CCD camera. Image processing together with a

calibration procedure allows visualizing directly the strain of the device as a function of time. Nanometric resolution in surface displacement is easily achieved, indicating how powerful such a technique can be in microelectronics.

Figure 1 shows the principle of the method. A sample is illuminated by coherent light from a laser source. An optical system  $\Sigma$  produces an image of the sample upon a CCD camera. As coherent light is used, the image is characterized by a speckle pattern (intense dots appear due to interference related to the roughness of the surface at light wavelength scale). To obtain the shearing interferometry, the optical system projects upon the CCD camera two identical images of the sample, slightly shifted one to another. For a better understanding, the 2 sheared images have been put in different planes in Figure 1. These two sheared images produce a new intensity distribution: the combination of the two images upon the CCD camera produces an interference pattern image where the intensity seen by a given pixel is related to the intensity of two points from the sample (distant by  $\Delta x$ ) and to their phase difference.

A calibration procedure allows to vary, in a controlled way, the phase difference of the two images at the CCD camera and to record the corresponding shearographs. This is done when no action or running is put to the sample. When the sample undergoes deformation, due to running for example, points from the surface move in the  $z$  direction. The shearograph evolves and contains information upon the relative  $\Delta z$  displacement between points separated by an amount  $\Delta x$ .

### 3 Strain localization.

Figure 2 illustrates what happens when surface displacement occurs. Let us consider 2 points of the sample surface at rest P and Q which image points are superimposed upon the CCD at point M. The two points on the sample are separated by the shear distance  $\Delta x$ . Their coordinates are  $P(x,y,z)$  and  $Q(x+\Delta x,y,z)$ . The mixing of the waves coming from P and Q produces an interference pattern at the detection plane, the intensity can be written:

$$I_{\text{rest}} = I_0 [ 1 + V \cos(\phi_{\text{sp}}) ]$$

where  $I_0$ ,  $V$  and  $\phi_{\text{sp}}$  are respectively the mean intensity of the laser, the interferometric contrast and the speckle phase at point M.

When the sample is stressed, strain appears and points P and Q move to P' and Q' which coordinates are

$P'(x+u,y+v,z+w)$  and  $Q'(x+\Delta x+u+\Delta u,y+v+\Delta v,z+w+\Delta w)$ . Values  $u,v$  and  $w$  are the  $P$  surface displacement vector components respectively along the  $x,y,z$  axis while  $u+\Delta u, v+\Delta v$  and  $w+\Delta w$  are the  $Q$  surface displacement vector components respectively along the  $x,y,z$  axis. For normal incidence, the illumination intensity pattern can be expressed:

$$I_{\text{stress}} = I_0 [ 1 + V \cos(\phi_{\text{sp}} + \Delta^x) ] \quad (5)$$

$$\text{with } \Delta^x = \frac{2\pi}{\lambda} \left( \frac{\partial u}{\partial x} \right) \Delta x. \quad (6)$$

A  $90^\circ$  rotation of the sample with respect to the optical axis of the system allows measuring the other component of phase shift:

$$\Delta^y = \frac{2\pi}{\lambda} \left( \frac{\partial u}{\partial y} \right) \Delta y. \quad (7)$$

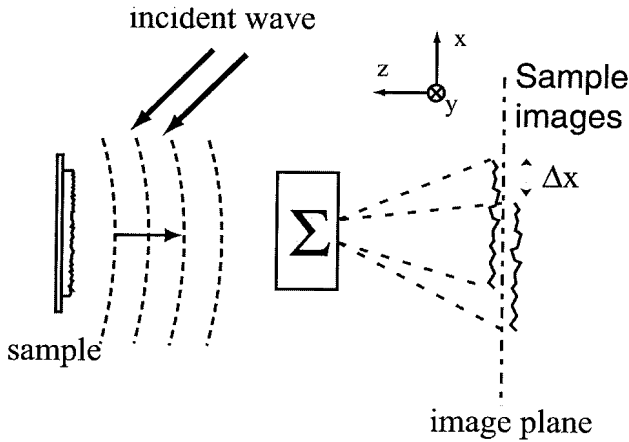


Figure 1: Schematic view of the shearography technique

When the shinning angle is not normal, the speckle intensity can be related to the component of the surface displacement ( $v$  and  $w$ ). Then one can determine the six following component of the strain tensor [6-7]

$$\frac{\partial u}{\partial x}, \frac{\partial v}{\partial x}, \frac{\partial w}{\partial x}$$

$$\text{and } \frac{\partial u}{\partial y}, \frac{\partial v}{\partial y}, \frac{\partial w}{\partial y}.$$

After determination of these strain tensor components we can calculate a fragility factor expressed by the following modulus:

$$g = \sqrt{\left(\frac{\partial u}{\partial x}\right)^2 + \left(\frac{\partial v}{\partial x}\right)^2 + \left(\frac{\partial w}{\partial x}\right)^2 + \left(\frac{\partial u}{\partial y}\right)^2 + \left(\frac{\partial v}{\partial y}\right)^2 + \left(\frac{\partial w}{\partial y}\right)^2} \quad (8)$$

This expression of fragility factor approximates the total deformation energy of the module.

#### 4 Optical set-up

The detailed optical set-up is schematized in Figure 3. The imaging system  $\Sigma$  produces 2 laterally shifted images. It is made of 2 lenses ( $L_2, L_3$ ), a Wollaston Prism ( $W$ ) and a sheet polarizer. The mirror ( $M$ ) (in dashed line in the figure) is

movable and allows shinning the sample either in normal incidence or in oblique incidence angle ( $\theta$ ). This is to obtain the different situations needed for the strain tensor determination.

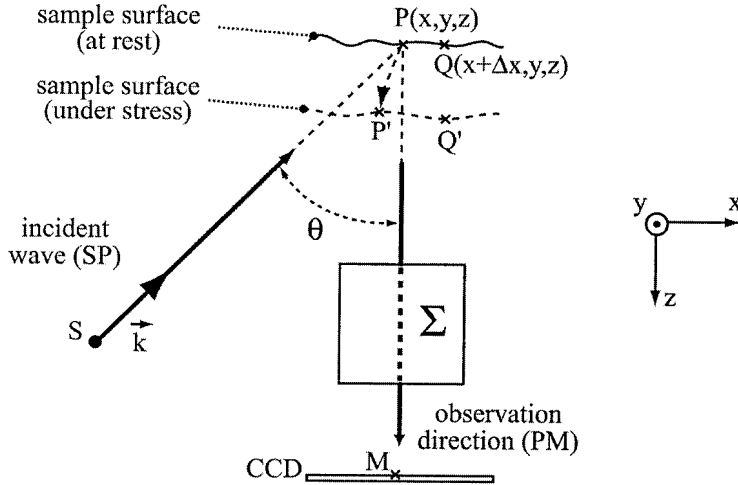


Figure 2: Principle of strain measurement

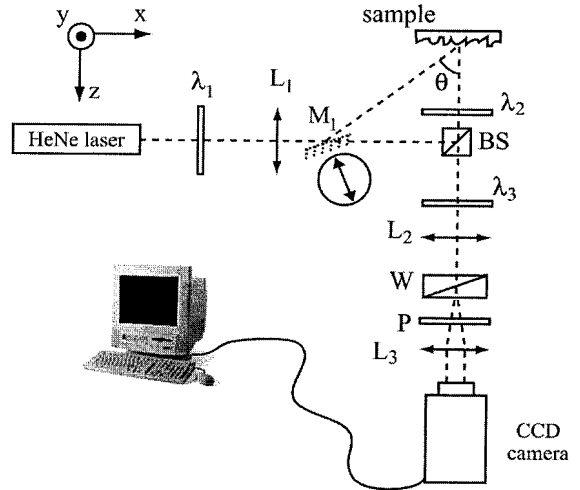


Figure 3: Optical set-up

The resolution is of the order of a few tens of nanometers with a lateral resolution of the order of the micrometer. The optical set-up is very robust with respect to vibrations and can be used in an industrial environment. Therefore this instrument is particularly well fitted to study thermoelectric devices.

#### 5 Sample

##### Thermoelectric cooler

The sample is a commercial thermoelectric cooler (by Melcor) presented in Figure 4. The device area is  $3 \times 3 \text{ cm}^2$ . Its maximum current is 9 A; maximum heat pump ability is 18.8W; maximum temperature difference between the hot and cold

surfaces is 70 °C. The sample is fed by an electrical current supply in closed loop control in order to keep a constant temperature difference between hot and cold faces. To monitor temperature a thermocouple is stuck in a corner of the device.

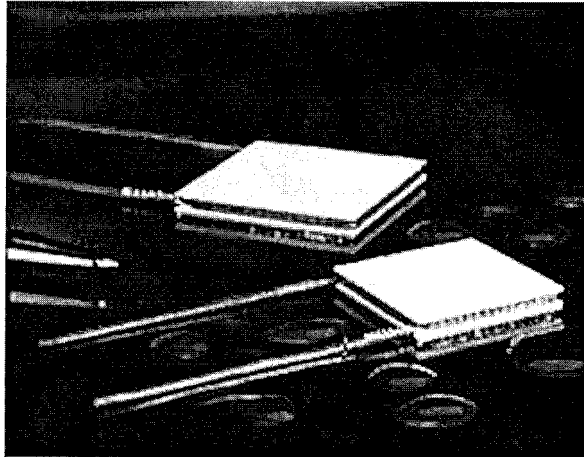


Figure 4: The thermoelectric module

### 6. Strain imaging of Thermoelectric module

The surface deformation of the cold face of the thermoelectric module has been analyzed. We present here two components of the strain measured by shearography. Figure 5

shows the  $\frac{\partial w}{\partial y}$  component of the strain tensor. This map was

obtained when a 1.35 K temperature difference was kept between faces, the hot-side surface is glued to a copper heat sink kept at room temperature. We have in purpose kept such a low temperature difference in order to show the performances of the optical bench.

Integrating the  $\frac{\partial w}{\partial y}$  map along the y axis allows

determining the normal surface displacement w. One can easily locate the maximum surface deformation in the middle of the face located at x=15mm. Two inflexion lines corresponding to the minimum and maximum values of the gradient are clearly visible.

A similar behavior can be seen on Figure 6 representing the  $\frac{\partial w}{\partial x}$  strain tensor component for the same conditions. Two

maximum strain lines appear revealing the inflexion lines in the surface deformation. We have also measured the 4 other components of the strain tensor and calculate the fragility factor (g). The result is presented in Figure 7. The maximum deformation energy is located around the central region of the cold face. One would expect some kind of 4 side symmetry. This is not completely true due probably to some fabrication process irregularities. As an example one corner is more expanding than

3/4

the others. The minimum value corresponds to the minimum temperature region of the Peltier cooler. The corner (x;y)=(30;30) undergoes also a strong deformation and a strong energy is concentrated in this area. This map allows determining the regions of the cooler which undergo the strongest stress during normal operating conditions.

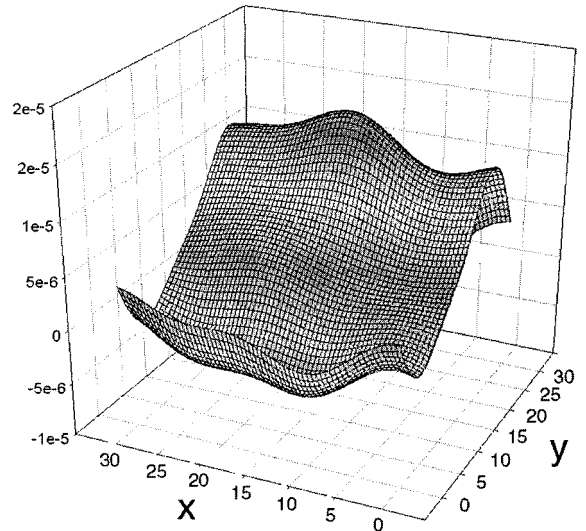


Figure 5: Map of deformation gradient  $\frac{\partial w}{\partial y}$  of cold-side alumina surface of a 30 × 30 mm<sup>2</sup> Peltier module.

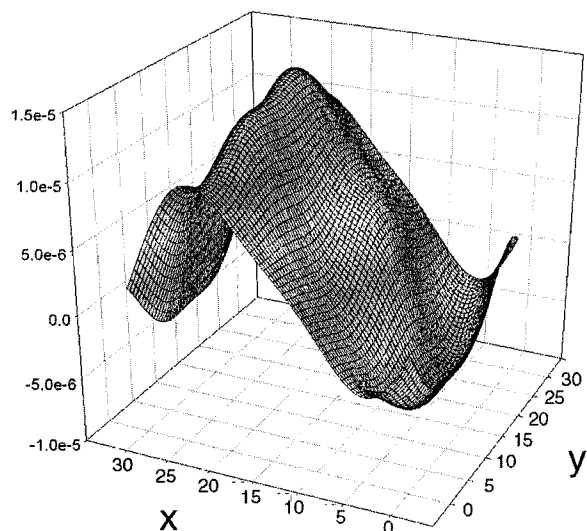


Figure 6: Map of deformation gradient  $\frac{\partial w}{\partial x}$  of cold-side alumina surface of a  $30 \times 30 \text{ mm}^2$  Peltier module.

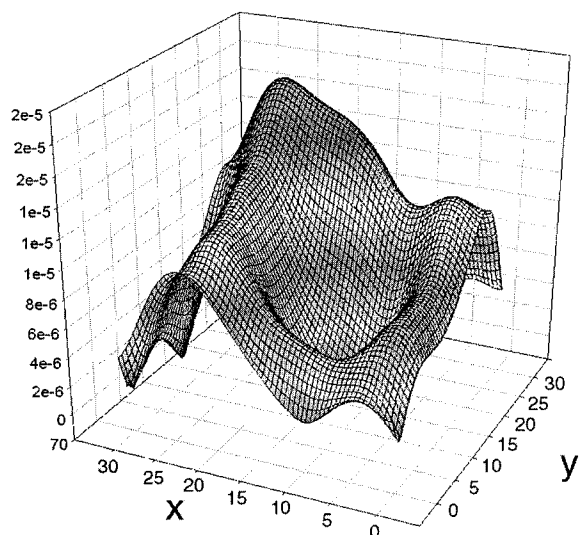


Figure 7: Map the fragility (g) factor of cold-side alumina surface of a  $30 \times 30 \text{ mm}^2$  Peltier module.

## 7. Conclusion

We have presented an original and powerful technique able to measure thermal induced strain in operating thermoelectric coolers. This method is a non contact, non destructive and low time consuming technique.

The well-marked result, even for such a low temperature difference, shows the high sensitivity of the optical bench. We are actually working on a numerical technique to calculate the stress tensor components from the strain measurement. The method allows analyzing at 25Hz the transient strain map.

## References

- [1] R. Jones and C. Wykes.  
Holographic and Speckle Interferometry.  
Cambridge University Press, second edition, 1989.
- [2] B Sharp.  
Electronic Speckle Pattern Interferometry (ESPI).  
Optics and lasers in engineering, (1989) vol. 11, pp 241-255.
- [3] Hung.  
Shearography: a new optical method for strain measurement and non-destructive testing  
Optical Engineering, (1982) vol. 21 n°3, pp 391-395.
- [4] S. W. James, R. P. Tatam.  
3D shearography for surface strain analysis.  
SPIE, vol. 3783 (1999).
- [5] S. Dilhaire, S. Jorez, L.D.Patino Lopez and W. Claeys.  
Measurement of the thermomechanical strain of electronic devices by shearography.  
Microelectronics Reliability 40, 1509-1514, 2000.
- [6] S. Dilhaire, S. Jorez, L.D.Patino Lopez and W. Claeys  
Optical method for the measurement of the thermomechanical behavior of electronic devices.  
Microelectronics reliability, (1999) vol. 39, pp 981-985.